MDPI

Article

Relationship between Phase Composition and Mechanical Properties of Peat Soils Stabilized Using Oil Shale Ash and Pozzolanic Additive

Ergo Rikmann [1] , Ivar Zekker [1,*], Tõnis Teppand [2], Vello Pallav [2], Merrit Shanskiy [3], Uno Mäeorg [1], Toomas Tenno [1], Juris Burlakovs [2] and Jüri Liiv [2]

[1] Institute of Chemistry, University of Tartu, 14a Ravila St., 50411Tartu, Estonia; ergo.rikmann@ut.ee (E.R.); uno.maeorg@ut.ee (U.M.); toomas.tenno@ut.ee (T.T.)

[2] Institute of Forestry and Rural Engineering, Estonian University of Life Sciences, 5 Fr. R. Kreutzwaldi St., 51006 Tartu, Estonia; tonis.teppand@emu.ee (T.T.); vello.pallav@emu.ee (V.P.); juris.burlakovs@emu.ee (J.B.); jyri.liiv@emu.ee (J.L.)

[3] Institute of Agricultural and Environmental Sciences, Estonian University of Life Sciences, 5 Fr. R. Kreutzwaldi St., 51006 Tartu, Estonia; merrit.shanskiy@emu.ee

* Correspondence: ivar.zekker@ut.ee; Tel.: +372-58194858

Abstract: Construction of road embankments in peatlands commonly involves replacement of the peat with a fill-up soil of an adequate load-bearing capacity. This usually requires a lowering of the water level, turning a peatland from a carbon sink to a source of greenhouse gases. Thus, alternatives are sought that are less costly in both economic and ecological terms. Mass-stabilization technology can provide a cheap substitute for Portland cement. Calcareous ashes (waste materials), supplemented with pozzolanic and alkali additives to facilitate and accelerate the setting and hardening processes, are attractive alternatives to soil excavation or replacement techniques. Silica fume and waterglass were used as pozzolanic agents and KOH as a soil-alkalizing agent. X-ray fluorescence (XRF), Fourier-transform infrared spectroscopy (FTIR), X-ray diffraction (XRD) analyses and stress–strain tests were performed for the hardened samples. Crystallization of alkali feldspars was observed in all test samples. Comparable hardening of peat soil was achieved for both ashes. It was shown that the ashes of Estonian kukersite (oil shale) from both pulverized firing and a circulating fluidized bed incineration process (produced in energy sector as quantitatively major solid waste in Estonia) can be used as binding agents for peat stabilization, even without the addition of Portland cement. Hardened peat soil samples behaved as a ductile material, and the cellulose fibers naturally present in peat gave the peat–ash composite plasticity, acting mechanically in the same way as the steel or glass fiber in ordinary reinforced concrete. The effect of peat fiber reinforcement was higher in cases of higher load and displacement of the composite, making the material usable in ecological constructions.

Keywords: soil stabilization; pozzolanic additive; humate; peat; oil shale ash

1. Introduction

Peatlands cover vast areas of the land surface, especially in the temperate and cold climate zones of the Northern Hemisphere, but they are also found in the hot regions. Peatlands cover 22% of the land area of Estonia [1,2]. Peat is highly compressible under high loading, which makes it one of the most difficult soils on which to construct buildings, roads, railroads, or other structures. Construction of large infrastructure in areas with loose peat soils often relies upon sophisticated building techniques.

To achieve an adequate load-bearing capacity of the roadbed, soil stabilization is usually required when a road or railway embankment will be constructed over a wetland area containing a peaty soil. The most common approach to the construction of road and rail track beds over peatlands is soil replacement [3]. This involves the excavation

and displacement of peat and sapropel, removal of the peat to reveal the bedrock layer, and then filling up the cavities with a material with a higher load-bearing capacity. Soil replacement is usually an expensive task since, in addition to the excavation work, it requires transportation of the displaced soil away from the site and the provision of a new soil and its transport to the site. The displaced material also requires disposal, which needs to be ecologically safe [4].

Excavation works typically require drainage of the surrounding wetland, leading to rapid decomposition of the peat deposits. As a result, the wetland switches from a carbon sink to become a net source of carbon dioxide emissions [1,5,6]. This excavation–displacement–replacement technique is considered feasible for peat deposits that are up to 5 m in peat depth. If the peat depth exceeds 3 m, the excavation and replacement costs will increase substantially [7]. In these deep excavations, the sideslopes become unstable and collapse into the excavations before they can be backfilled. To avoid this problem, large volumes of soil need to be removed from the sideslopes to ensure that the slope angle does not exceed the wet soil's critical angle of repose, thus increasing the total volume of the excavation work. Moreover, the excavation area requires installation of its own drainage system, thus further damaging the drainage regime and overall hydrology of the area [8,9] and potentially further increasing CO_2 emissions [1]. Moreover, removed soil needs be transported from the site for use in landscaping in the adjacent areas, further increasing the costs. These problems highlight the need to develop functional, cost-effective, and environmentally sound methods for stabilizing embankments over peatland areas.

Economic and environmental impact can be met when an in situ soil reinforcement technique, such as mass stabilization, is applied. To achieve mass stabilization, the peat soil is mixed with a dry or a wet binder and additives ($CaCl_2$, $Al_2(SO_4)_3$, or SiO_2) throughout the volume of the treated soil column. Common binders include Portland cement, quicklime, and gypsum [3,10]. Environmentally sustainable waste-based binders applied for stabilization of various soils (peaty, clayey or sandy soils) may include calcareous fly ashes [11], carbide lime [12], or phosphogypsum [10]. In order to facilitate the hardening of the soil-binder mixture, pozzolanic agents like silica fume, waterglass, alumino-siliceous fly ash, granulated blast furnace slag, ground glass, bentonite, kaolin, or other siliceous and alumino-siliceous materials can be used [3,9,10,13]. Soluble calcium or aluminum salts such as $CaCl_2$ or $Al_2(SO_4)_3$ can be added as supplementary Ca and Al sources [9,10,13,14]. Peat soils contain a high percentage of organic material and few to no solid mineral particles. Therefore, within the mass stabilization process the addition of granular filler materials, such as sand or inert construction wastes (e.g., recycled asphalt pavement or crushed bricks), to the mixture allows cementitious compounds to carry out a pozzolanic reaction, or from the hydration of cement to bind the particles together, enhancing the strength of the stabilized peat [12,14,15].

Humic and fulvic acids in the peat hinder the setting and hardening of cement pastes, which occurs for several reasons [7]. Adsorption of insoluble calcium and magnesium humates onto the binder particle surfaces, and additive materials interfere with the hydration of calcium silicates and aluminates, which slows down pozzolanic reactions. Moreover, fulvic acids selectively associate with aluminum-bearing mineral particles, inhibiting the hydration of aluminates and impeding crystallization hydration products [14]. Leaching of organic acids from peat may reduce the pH of the mixture, decreasing the solubility of siliceous species and therefore hindering formation of calcium (aluminum) silicate hydrate (C(A)SH) gels [7,16]. If the pH of the pore water is below 9, secondary cementation products cannot form [17]. A high ratio of organic to mineral in peat implies a high water-retention capacity and a high moisture content, which results in a high water-to-binder ratio that, in turn, limits any increase in the strength of the mixture. In the case of peat soils, this combination of a high organic content, a lack of pozzolanic and solid inert particles, an acidic media (primarily from humic and fulvic acids), and a high water-to-solids ratio impedes the efficient hydration of cement and hinders any subsequent increase in the compressive strength of the soils [14]. The compressive strength and content of hydration

products in the soil–cement mixture decreases until a certain threshold value of humic matter is achieved, beyond which the additional humic matter has a limited effect on the mixture's compressive strength [18].

The cost-efficiency of the mass stabilization technology can be improved using a cheap substitute for cement or lime. In Estonia, kukersite oil shale ash can be used for this purpose. Oil shale ash has been used in a mixture with Portland cement in Estonia for road construction using the mass stabilization technique and could also be used in peaty areas [11]. Earlier studies have concluded that ash from a circulating fluidized bed (CFB) firing process would need a sophisticated approach for use as a binder agent for the soil stabilization purposes, because of its low free lime content and low pozzolanic activity [16]. The CFB firing is a newer technology for incineration of kukersite oil-shale in Estonian thermal power plants. Therefore, different soil mass stabilization and other approaches are needed to make CFB ash recovery more efficient. Mass stabilization technology would be successfully applied by using CFB ash and peat. This hypothesis is also based on the experience of development of an environmentally friendly peat–ash composite building material [16].

In this study, peat soil samples from south Estonia were mixed with different oil shale samples, pozzolanic additives and potassium hydroxide. Subsequently, X-ray diffraction analyses (XRD), X-ray fluorescence spectroscopy (XRF), and Fourier-transform infrared spectroscopy (FTIR) analyses were conducted, and stress–strain diagrams for compression were created to prove the suitable chemical content and hardness of the material. We aim to show that the hardened peat composite is a ductile material and that peat fibers behave like steel reinforcement. In this study, we hypothesized that all forms of oil shale ashes can be used as binders for organic soils in a cost-effective and environmentally sound way, based on addition of pozzolanic agents with high chemical activities, and an increase in the pH of the pore water in the organic soil-binder mixture using addition alkali metal hydroxides. Mass stabilization technology has the potential to be applied by using hazardous waste, CFB ash, and peat in composite material.

2. Materials and Methods

We tested different mixtures of peat soil from south Estonia, and oil shale ashes with various siliceous additives, and selected three mixtures with substantially different properties for further detailed studies of the concrete compositions and compressive strength.

For the preparation of laboratory samples, 200 g of peat soil was mixed with different additives. Additives from pulverized firing (PF; T10 and T17) or circulating fluidized bed (CFB) firing (T11) of kukersite oil shale in the power plant of Eesti Energia were used. As pozzolanic agents, silica fume (Efaco, Egypt), and Na_2SiO_3 (20% solution) were used, and KOH was added to some samples to increase the pH value of the mixture. The compositions of the mixtures from the analyzed test pieces are given in Table 1.

Table 1. List of samples and different used phases and their mass concentrations.

Test Piece	Peat Soil, g	CFB Ash, g	PF Ash, g	Silica Fume SiO_2, g	Na_2SiO_3 20% Solution, g	KOH, g
T10	200	0	100	100	100	0
T11	200	100	0	50	30	30
T17	200	0	200	50	30	30

The XRD analysis was performed on a diffractometer SmartLabTM (Rigaku, Tokyo, Japan) using a Cu rotating anode working at 45 kV and 180 mA, a coordinate-sensitive 1D detector D/teX Ultra, and a Bragg–Brentano optical setup. The diffraction pattern was measured between diffraction angles of 8° and 90°, with a step size of 0.01° (2θ) and a scan speed of 4° min^{-1}. PDXL (Rigaku) software and the PDF-2 (International Centre of Diffraction Data, 2018) database were used for phase identification, and TOPAS 6 Academic

software was used for the Rietveld analysis. The Rietveld analysis involves the fitting of a complete experimental diffraction pattern with calculated profiles and background.

The XRF analysis was performed on spectrometer ZSX 400 (Rigaku, Japan) using an Rh X-ray tube working at 3 kW.

One-axis compressive tests were carried out on an Instron Universal Testing Machine (Model 3369; max load 50 kN). Samples were weighed with a Kern 578 electronic balance (d = 0.05 g) before the tests. The surfaces of loaded test samples were flattened and ground, so that the difference in the surface smoothness did not exceed 0.1 mm per 100 mm side length, and were then supported on the loading plates evenly. The loading on the test pieces was applied by continuously increasing force until breaking or exact displacement of 16 mm. Subsequently, the maximum force was recorded. The compressive strength f_c (N mm^{-2}) was calculated as a quotient of F_c (N), maximum compression force, and the gross area of loaded surface (mm^2). The mean compressive strength was calculated as the arithmetic mean of the sum of the single specimen with the accuracy of 0.1 N mm^{-2}. The FTIR spectra were measured by Spectrum GXII (Perkin Elmer) spectrometer with an ATR (ZnSe) device (Interspectrum OÜ, Tartu, Estonia) to assess the chemical bonds within the composition of the samples.

3. Results

3.1. Composition of Oil Shale Ashes

Unlike coal fly ash, oil shale ash is non-pozzolanic in nature because of its high CaO and low SiO$_2$ and Al$_2$O$_3$ contents. It also has a high content of alkali metals, which contributes to a high alkalinity. The main types of oil shale ashes released are CFB ash (from the first field of electrostatic precipitators of a boiler operating on the CFB incineration principle), ash from pulverized firing (PF) collected from cyclones or electrostatic precipitators, and deSOx ash (from desulfurization unit of flue gases for a boiler operating on the PF principle). The mineral compositions of the oil shale ash are shown in Table 2.

Table 2. Mineral composition of the oil shale ash.

Mineral	PF Cyclone Ash Mass Concentration (%)	CFB I Filter Ash Mass Concentration (%)
Quartz, SiO$_2$	3.3	16.8
Orthoclase, KAlSi$_3$O$_8$	1.7	12.5
Illite+Illite-Smectite, Na,K$_x$(Al,Mg)$_2$Si$_4$O$_{10}$(OH)$_2$×H$_2$O	6.1	13.8
Belite, Ca$_2$SiO$_4$	15.9	5.3
Merwinite, Ca$_3$Mg(SiO$_4$)$_2$	13.2	3.7
C$_3$A, 3CaO·Al$_2$O$_3$	2.2	2.3
Pseudowollastonite, CaSiO$_3$	1.6	3.6
Periclase, MgO	8.7	2.7
Melilite, (Ca,Na)$_2$(Mg,Al)(Si,Al)$_3$O$_7$	5.8	1.2
Anhydrite, CaSO$_4$	5.4	9.5
Lime, CaO	29.3	10.8
Calcite, CaCO$_3$	2.5	13.5
Portlandite, Ca(OH)$_2$	3.1	nd
Hematite, Fe$_2$O$_3$	1.1	4.3

3.2. Stress–Strain Tests

The stress–strain curves of the hardened soil samples have a characteristic shape for ductile material (Figure 1). This is dissimilar to concrete, which is a brittle material. Natural peat cellulose fibers give peat-ash composite plasticity. The compressive strengths of the three peat–ash composites that were studied are shown in Table 3.
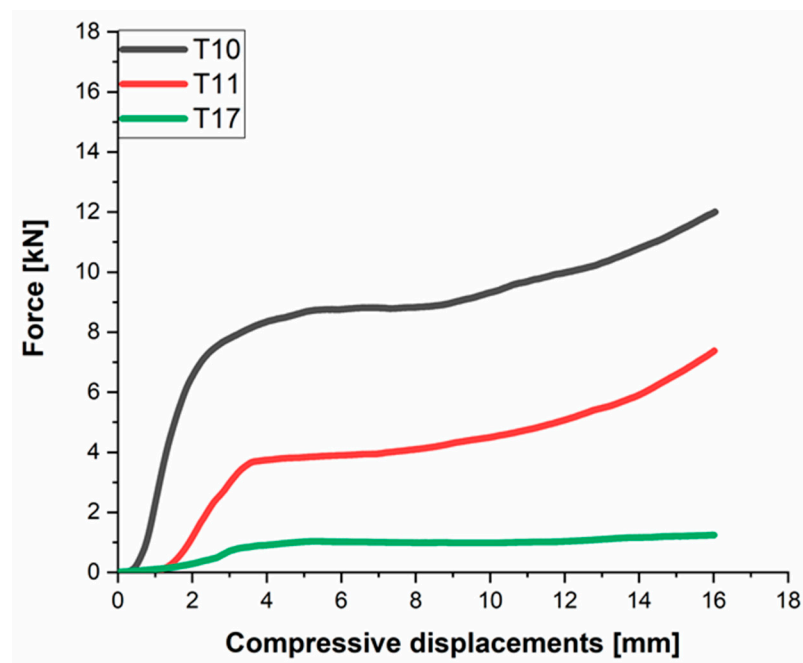
Figure 1. Compressive test diagrams for the three tested composites.

Table 3. The compressive strengths of the samples from each of the three studied peat–ash composites.

Sample	1st Parallel, N mm^{-2}	2nd Parallel, N mm^{-2}	3rd Parallel, N mm^{-2}	4th Parallel, N mm^{-2}	5th Parallel, N mm^{-2}
T10	1.62	1.55	1.60	1.65	1.58
T11	0.99	0.95	1.00	0.99	1.02
T17	0.20	0.17	0.16	0.15	0.17

For the sake of conciseness following, there were presented average values for the stress–strain curves.

Further details of the measured compressive displacements and strengths of test pieces shown in Figure 1 are presented in Table 4. The maximum force required to achieve a maximum compressive displacement of 16 mm was 12.01 kN for T10, 7.38 kN for T11, and 1.25 kN for T17. The retention time of all test pieces at maximum force was 480 s (Table 5). The maximum force correlated positively with the content of crystalline phases in the samples.

Tests showed the mixture of CFB and PF ashes formed building materials with some good compressive properties (Table 4) and suitable chemical composition (Table 5).

Table 4. Compressive displacements and strength of the three tested composites.

Specimen	Thickness (mm)	Diameter (mm)	Specific Weight (kN m^{-3})	Compressive Displacement at Maximum Force (mm)	Maximum Force (kN)	Time at Maximum Force (s)	Compressive Strength (N mm^{-2})
T10	41.29	97.71	132.90	16.04	12.01	481.26	1.60
T11	34.57	97.56	142.80	16.02	7.38	480.56	0.99
T17	49.89	95.41	145.16	16.01	1.25	480.26	0.17

Table 5. Elemental composition of crystalline phases of test pieces as mass percentages (±represents standard deviation between replicate measurements (*n* = 3)).

Chemical Element	T10	T11	T17
Al	1.607 ± 0.046	1.252 ± 0.057	0.552 ± 0.036
C	0.808 ± 0.018	1.272 ± 0.043	0.819 ± 0.020
Ca	6.912 ± 0.198	15.960 ± 0.227	19.666 ± 0.110
Cl	0.108 ± 0.021	0.349 ± 0.039	0.085 ± 0.026
Fe	0.319 ± 0.038	0.849 ± 0.036	0.343 ± 0.048
K	3.655 ± 0.065	4.309 ± 0.128	3.296 ± 0.060
Mg	0.071 ± 0.017	1.187 ± 0.055	1.153 ± 0.035
Na	0.340 ± 0.016	0.092 ± 0.014	0.069 ± 0.012
O	50.562 ± 0.036	48.945 ± 0.083	49.409 ± 0.046
S	0.782 ± 0.010	1.089 ± 0.030	1.035 ± 0.014
Si	34.836 ± 0.128	24.696 ± 0.072	23.572 ± 0.070

3.3. XRD-XRF Analyses of Crystalline Phases

The elemental composition of crystalline phases was determined by a Rietveld analysis (Table 5). Si and Al presence indicate the pozzolanic reaction taking place and proving formation of CSH material.

The CFB ash was able to form a high-strength material, which was intended to be shown during experiments. The Na_2SiO_3 20% solution and silica fume addition to the PF ash at 100 g for sample T11 produced the highest shear strength among the test samples. Furthermore, CFB ash showed relatively high shear strength, exceeding the values of PF ash performed at equal amounts of silica fume and 30 g of Na_2SiO_3 20% solution.

The identified phases and their mass concentrations are given in Table 6. The probability of identification of phases for which concentration is below 1 mass percent was below 100%. The phase "CSH, semi-amorphous" was assumed to be present in the sample, and its parameters were included in the calculations.

Table 6. List of represented phases and their mass concentrations (%) for samples. Rwp and Rwp' represent measuring errors including and excluding background, respectively. The highest uartz, (SiO_2) content for sample 10 is shown in bold.

Name of Phase	T10 Rwp = 2.9%; Rwp' = 9.2%	T11 Rwp = 2.4%; Rwp' = 12.4%	T17 Rwp = 2.7%; Rwp' = 15.7%
	Mass Concentrations, %		
Quartz, SiO_2	33.6(1)	10.3(1)	6.8(1)
Calcite, $CaCO_3$	4.0(1)	5.0(1)	3.7(1)
Feldspar, $K(AlSi_3O_8)$	1.4(2)	1.4(2)	1.1(1)
Orthoclase, $K(AlSi_3O_8)$	2.3(1)	3.8(2)	1.1(1)
Microcline, $(K,Na)(AlSi_3O_8)$	4.1(2)	1.3(2)	0.7(1)
Albite, $Na(AlSi_3O_8)$	2.2(1)	0.5(1)	0.4(1)
Arcanite, $K_2(SO_4)$	2.6(1)	3.2(1)	3.3(1)
Dolomite, $CaMg(CO_3)_2$	–	0.7(1)	–
Hematite, Fe_2O_3	–	0.7(1)	0.3(1)
Akermanite, $Ca_2MgSi_2O_7$	–	2.2(1)	0.4(1)
Periclase, MgO	–	0.6(1)	1.0(1)
Belite (larnite), $Ca_2(SiO_4)$	–	–	2.4(1)
CSH (calcium silicate hydrate), semi-amorphous	10(1)	24(2)	37(1)
Amorphous phase (external standard method)	40(1)	46(2)	42(1)

3.4. FTIR Spectra Analyses

The FTIR spectra of studied samples are shown in Figure 2. Since the materials studied are composites from different compounds, only general assignment is possible. For all samples, the most intensive bands in the 1000 cm^{-1} region belong to different Si-O

stretching vibrations and contain the signals from alkali and alkaline earth metal silicates. The characteristic absorption band at 966 cm^{-1} belongs to Si-O-M, indicating the presence of silicates in sample T17. Silica (foam), absorbing at 1070 cm^{-1} and 800 cm^{-1}, was not present, or was present at very low concentrations overlapping with silicate maxima. The signal at 1116 cm^{-1} in the same sample could correspond to the silicic acid. The maxima at 1400 cm^{-1} and 870 cm^{-1} could be assigned to the carbonates of different metals in different crystalline forms. Signals at 3300–3400, 1635, and 700 cm^{-1} were attributed to absorbed water.
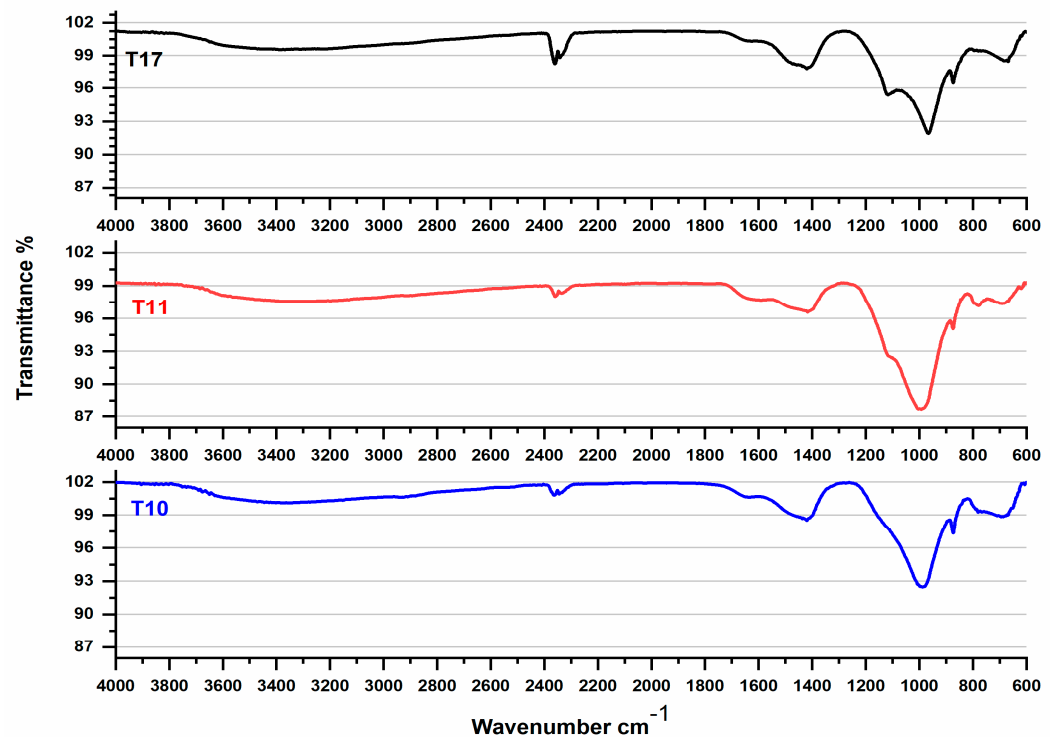

Figure 2. Fourier-transform infrared spectroscopy (FTIR) spectra analyses of the test pieces.

4. Discussion

It could be proposed that fibers naturally present in peat act mechanically in the same way as the steel or glass fiber in ordinary concrete, with the difference under compression showing the differences in strength (Table 3). The reinforcement and non-loosing plasticity provided by peat fiber is better when the load is higher on the peat-ash composite and the displacement is lower. Figure 1 shows that the composite compressive strength increases again, unlike the ordinary concrete. This may be because increasing heat from pressure acts together with lignin from the fibers naturally present in peat, providing an additional gluing effect inside the composite. This phenomenon needs to be further explored.

As shown in Table 6, the content of the semi-amorphous CSH phase almost quadrupled in the sequence T17 > T11 > T10, whereas non-hydrated quartz followed the diametrically opposite trend. Quartz content showed decrease from 33.6 to 10.3 and 6.8% between tests T10 > T11 > T17, respectively. The high SiO$_2$ content in T10 also shows that SiO$_2$ was added in excess and its hydration and inclusion into CSH gel was Ca-limited, resulting in lower plasticity compared with the other samples. For T10 and T11, which had a smaller CSH paste content, the crystallization of alkali feldspars progressed more rapidly, whereas it was delayed in T17. The crystallization of alkali feldspars has also been observed in our previous work aiming to produce 3D-printable peat-ash composite construction material [16]. The full-amorphous phase (which includes both organic matter as well as a fraction of CSH paste) was relatively evenly presented among all samples. Belite was present in T17 only. The crystalline phases of T11, which contains CFB ash, also showed

a higher content of Mg-and Fe-bearing minerals. Calcium silicate hydrate (CSH) is the main and most important constituent of cement paste (and pastes formed in the reaction of lime with siliceous agents). Its hydration forms most of the new solid phases that give hardened cement paste its strength. It occupies approximately 50% of the paste volume and responds to nearly all the engineering properties of the cement paste [18]. Related equilibrium studies have been performed assessing the effect of pH and other factors on the material performance [19–21].

5. Conclusions

The results of this study reveal that ashes from the PF and CFB processes can be applied as a cheap and widely available binder for the stabilization of peat columns, without any addition of Portland cement, when pozzolanic additives such as silica fume and waterglass and alkali pH modifiers are used. Further studies are needed to optimize the quantity of ash and additives, and to explore whether cheaper waste-based pozzolanic and alkali additives could be used. The XRD-XRF analyses of the test samples revealed that alkali feldspars were formed during the end hardening, whereas crystallization of belite and the other calcium silicates was a slower process. Stress–strain curves of hardened peat soil composites revealed that the composites behaved as ductile materials and herbal fibers in the peat increased their plasticity, allowing them to act mechanically in the same way as steel or glass fiber in ordinary concrete under high compression. The higher the load on the peat-ash composite during displacement, the better the fiber naturally present in peat reinforces it with non-loosing plasticity. This is probably due to the increased heat emanating from the pressure affecting lignin of herbal fibers, which results in an additional gluing effect inside the composite. This phenomenon needs to be further explored for production of novel ecological composites.

Author Contributions: Conceptualization, E.R. and J.L.; methodology, E.R.; software by T.T. (Toomas Tenno); validation, M.S.; formal analysis, V.P.; investigation: E.R. and I.Z.; resources, T.T. (Tõnis Teppand); data curation, I.Z.; writing—original draft preparation, J.L.; writing—review and editing, E.R.; visualization, I.Z.; supervision, J.L.; project administration, V.P., U.M., J.B.; funding acquisition, T.T. (Toomas Tenno). All authors have read and agreed to the published version of the manuscript.

Institutional Review Board Statement: Not applicable.

Informed Consent Statement: Not applicable.

Data Availability Statement: Not applicable.

Conflicts of Interest: The authors declare no conflict of interest. The funders had no role in the design of the study; in the collection, analyses, or interpretation of data; in the writing of the manuscript, or in the decision to publish the results.

References

1. Liiv, J.; Zekker, I.; Tämm, K.; Rikmann, E. Greenhouse gases emissions and climate change—Beyond mainstream. *MOJ Bioorg. Org. Chem.* **2020**, *4*, 10–16. [CrossRef]
2. Orru, M.; Orru, H. Sustainable use of Estonian peat reserves and environmental challenges. *Est. J. Earth Sci.* **2008**, *57*, 87. [CrossRef]

3. Axelsson, K.; Johansson, S.-E.; Andersson, R.; Djupstabilisering, S. Stabilization of Organic Soils by Cement and Puzzolanic Reactions-FEASIBILITY STUDY English Translation. 2002. Available online: http://www.swedgeo.se/sd.htm (accessed on 12 January 2020).
4. Vasander, H.; Tuittila, E.-S.; Lode, E.; Lundin, L.; Ilomets, M.; Sallantaus, T.; Heikkilä, R.; Pitkänen, M.-L.; Laine, J. Status and restoration of peatlands in northern Europe. *Wetl. Ecol. Manag.* **2003**, *11*, 51–63. [CrossRef]
5. Gorham, E. Northern Peatlands: Role in the Carbon Cycle and Probable Responses to Climatic Warming. *Ecol. Appl.* **1991**, *1*, 182–195. [CrossRef] [PubMed]
6. Limpens, J.; Berendse, F.; Blodau, C.; Canadell, J.G. Peatlands and the carbon cycle: From local processes to global implications—A synthesis. *Biogeosciences* **2008**, *5*, 1475–1491. [CrossRef]
7. Zulkifley, M.T.M.; Ng, T.F.; Raj, J.K.; Hashim, R.; Bakar, A.F.A.; Paramanthan, S.; Ashraf, M.A. A review of the stabilization of tropical lowland peats. *Bull. Eng. Geol. Environ.* **2014**, *73*, 733–746. [CrossRef]
8. Munro, R. Dealing with Poor Bearing Capacity on Low Volume Roads on Peat in the Northern Periphery. 2005. Available online: www.peatlandsni.gov.uk (accessed on 4 March 2005).
9. Huat, B.B.K.; Kazemian, S.; Kuang, W.L. Effect of cement-sodium silicate grout and kaolinite on undrained shear strength of reinforced peat. *Electron. J. Geotech. Eng.* **2020**, *16*, 1221–1228.
10. Moayedi, H.; Huat, B.B.K.; Kazemian, S.; Daneshmand, S. Stabilization of organic soil using sodium silicate system grout. *Int. J. Phys. Sci.* **2012**, *7*, 1395–1402. [CrossRef]
11. Reinik, J.; Irha, N.; Koroljova, A.; Meriste, T. Use of oil shale ash in road construction: Results of follow-up environmental monitoring. *Environ. Monit. Assess.* **2018**, *190*. [CrossRef]
12. Consoli, N.C.; Carretta, M.d.; Leon, H.B.; Filho, H.C.S.; Tomasi, L.F. Strength and Stiffness of Ground Waste Glass–Carbide Lime Blends. *J. Mater. Civ. Eng.* **2019**, *31*, 06019010. [CrossRef]
13. Wong, L.S. Formulation of an optimal mix design of stabilized peat columns with fly ash as a Pozzolan. *Arab. J. Sci. Eng.* **2015**, *40*, 1015–1025. [CrossRef]
14. Wong, J.K.H.; Kok, S.T.; Wong, S.Y. Cementitious, Pozzolanic And Filler Materials For DSM Binders. *Civ. Eng. J.* **2020**, *6*, 402–417. [CrossRef]
15. Dehghanbanadaki, A.; Arefnia, A.; Keshtkarbanaeemoghadam, A.; Ahmad, K.; Motamedi, S.; Hashim, R. Evaluating the compression index of fibrous peat treated with different binders. *Bull. Eng. Geol. Environ.* **2017**, *76*, 575–586. [CrossRef]
16. Liiv, J.; Teppand, T.; Rikmann, E.; Tenno, T. Novel ecosustainable peat and oil shale ash-based 3D-printable composite material. *Sustain. Mater. Technol.* **2018**, *17*, e00067. [CrossRef]
17. Tremblay, H.; Duchesne, J.; Locat, J.; Leroueil, S. Influence of the nature of organic compounds on fine soil stabilization with cement. *Can. Geotech. J.* **2002**, *39*, 535–546. [CrossRef]
18. Ma, C.; Chen, B.; Chen, L. Effect of organic matter on strength development of self-compacting earth-based construction stabilized with cement-based composites. *Constr. Build. Mater.* **2016**, *123*, 414–423. [CrossRef]
19. Tenno, T.; Rikmann, E.; Zekker, I.; Tenno, T. Modelling the solubility of sparingly soluble compounds depending on their particles size. *Proc. Est. Acad. Sci.* **2018**, *67*, 300–302. [CrossRef]
20. Zekker, I.; Tenno, T.; Selberg, A.; Uiga, K. Dissolution Modeling and Experimental Measurement of CaS-H_2O Binary System. *Chin. J. Chem.* **2011**, *29*, 2327–2336. [CrossRef]
21. Tenno, T.; Rikmann, E.; Uiga, K.; Zekker, I.; Mashirin, A.; Tenno, T. A novel proton transfer model of the closed equilibrium system $H_2O–CO_2–CaCO_3–NH_X$. *Proc. Est. Acad. Sci.* **2018**, *4017*, 2. [CrossRef]